Friction and Wear Behavior of Titanium Matrix Composite Reinforced with Carbon Nanotubes under Dry Conditions†

THRERUJIRAPAPONG Thotsaphon*, KONDOH Katsuyoshi, UMEDA Junko*** and IMAI Hisashi*****

Abstract

The friction and wear behavior of multi-wall carbon nanotube (MWCNT)-reinforced Ti composite were evaluated under dry sliding conditions. Ti powders were immersed in suspended 3.0wt.% MWCNTs in a zwitterionic surfactant solution to prepare the composite. To eliminate the solid zwitterionic substance, coated Ti powders were heated at 873 K for 3.6 ks under a mixed H_2/Ar gas atmosphere. Coated Ti powders were mixed with pure Ti powders at ratios of 0, 20, 50 and 100 in wt.%. Spark plasma sintering and hot compression were applied to consolidate the mixed powders. Subsequently, a ball-on-disk test was carried out at a rotational speed of 120 rpm with different applied loads of 0.98, 1.96 and 2.94 N by using 304 stainless steel balls as a counter material. The friction coefficient of each specimen decreased with increasing MWCNT content and applied load.

KEY WORDS: (Titanium) (Carbon Nanotube) (Friction coefficient) (Powder metallurgy) (Hot compression)

1. Introduction

Since the first observation of multi-wall carbon nanotubes (MWCNTs) reported by S. Iijima[1] , MWCNTs have drawn interest in various research fields because of their excellent properties[2-3]. Many researchers have shown that MWCNT-reinforced metal composites have greatly enhanced yield strength, tensile strength and hardness[4-8]. However, there are a few reports of tribological behavior of metals reinforced with MWCNTs for structural applications[9-11]. Cumings and Zettle[12] revealed the slip phenomenon of MWCNTs where the outer and inner shells of the nanotube could be easily extracted without any damage. This led to the design of low friction bearing applications at the nanoscale. With regard to the application at higher scale levels, a previous study[10] showed the effectiveness of MWCNTs coated on the Ti-6Al-4V alloy. Wear resistance of coated materials improved because the contact between the pin and disk was protected by the remaining MWCNTs during testing. In this study, friction behaviors of pure Ti reinforced with MWCNTs at different applied loads were investigated. It was expected that MWCNTs would be effective in improving the tribological behavior of pure Ti.

2. Experimental

2.1 Sample Preparation

Commercially pure Ti powders, having a mean particle size of 30 μm, were used as the matrix. The chemical analysis of raw Ti powders was Fe 0.03, Si 0.01 Mg <0.001, Cl <0.002, O 0.21, N 0.02, C <0.01 in wt.%. Multi-wall carbon nanotubes (Nanocyl S.A.) with an average diameter of 9.5 nm and length of 1.5 μm were used as the reinforcement. The zwitterionic surfactant solution with 3.0wt.% MWCNTs was employed in this experiment. The zwitterionic surfactant comprises both hydrophobic and hydrophilic functional groups that effectively overcome the van der Waals forces between MWCNTs[13]. Therefore, MWCNTs were dispersed individually in the zwitterionic surfactant solution. Ti

† Received on December 26, 2008
* Graduate Student
** Professor
*** Specially Appointed Researcher

Transactions of JWRI is published by Joining and Welding Research Institute, Osaka University, Ibaraki, Osaka 567-0047, Japan

powders were immersed into the aqueous MWCNT/zwitterionic solution and subsequently dried in a furnace at 373 K for 10.8 ks. To eliminate the solid zwitterionic substance, dried Ti powders were heated in a horizontal tube furnace at 873 K for 3.6 ks under a mixed H_2/Ar gas atmosphere. Composite Ti powders coated with nanotubes were obtained and mixed with un-coated Ti powders in weight ratios of 0, 20, 50 and 100wt.%. These elemental mixture powders were designed as 0C, 20C, 50C and 100C, respectively. They were consolidated by a spark plasma sintering (SPS, Syntech Co. SPS-103S) process at 1073K for 1.8 ks under vacuum atmosphere. The applied load during the process was 41 kN. The sintered Ti billet was heated to 1273 K for 180 s under an Ar atmosphere, immediately followed by compression in the closed die. The compression load and holding time were 1600 kN and 10s. The compression mold temperature was kept at 673 K. Finally, the hot-compression billets were machined to disk-shaped specimens with a diameter of 40 mm, height of 10 mm, and a surface roughness, Ra, lower than 0.1 μm for the friction test specimens.

2.2 Ball-on-disk test

Friction tests were evaluated using 4.76 mm-diameter 304 stainless steel (SUS304) balls in a ball-on-disk machine (RHESCA Co Ltd., FPR-2100 model) under laboratory atmosphere. Tests were carried out at a rotational speed of 120 rpm with a track radius of 5 mm (equivalent to surface sliding speed of 62.83 mm/s) under the normal applied load of 0.98, 1.96 and 2.94 N. The frictional torque during testing was automatically recorded. The friction coefficient was calculated from the results of the frictional torque between the SUS304 ball and the Ti composite disk specimen.

2.3 Characterization

The density of each hot-compressed billet was determined by the Archimedes method. The hardness of each was measured by a micro-Vickers hardness tester (Mitutoyo). Wear surface was investigated by optical and scanning electron microscopes (SEM, Hitachi SU-70) equipped with EDS. Microstructures of the wear track and debris were characterized using a locally selected area X-ray diffractometer (XRD, Bruker-D8) using CoKα1 radiation (wavelength 1.78897 Å)

3. Results and Discussion

3.1 Samples characterization

The morphologies of the obtained Ti powders after eliminating the solid zwitterionic substance are shown in **Fig.1**. Close observation of the marker in **Fig. 1(a)** indicates that un-bundled MWCNTs are individually separated and uniformly dispersed on the Ti powder surface (**Fig. 1(b)**). This is an ideal morphology for the powder in composite processing.

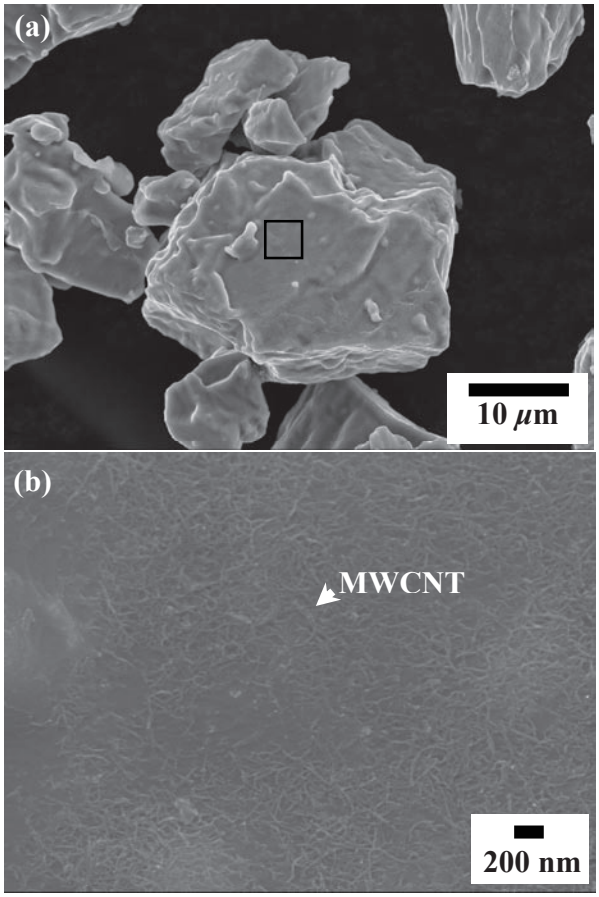

Fig.1 Fine Ti powder coated with MWCNTs (a) and uniformly dispersed un-bundled MWCNTs on the Ti powder surface (b).

The measured density of each sample is listed in **Table 1**. Regarding the relative density of each sample, the theoretical value for each Ti composite was calculated based on a rule of mixtures. The hot-compressed titanium composites sample showed the remaining MWCNTs and TiC compounds in their microstructures. The calculation was made assuming no reaction between Ti and MWCNTs because the volume fraction of the remaining MWCNTs and TiC compounds could not be measured exactly. The assumption also neglected the effect of in-situ formed titanium hydride compounds since there was no significant difference between their theoretical densities (4.50 g•cm-3 [14] versus 4.51 g•cm-3 [15] for Ti). The theoretical percentage showed values over 95%, which means that the processing could be used effectively to prepare highly dense MWCNT/Ti composite materials. The effect of pores on the friction test was neglected.

Table 1 Carbon content, relative densities, hardness and surface roughness of each specimen.

Specimen	Carbon content	Density[1]	Calculated density[2]	Relative density	Ra	Surface Hardness	Bulk Hardness	
	(wt.%)	($g \cdot cm^{-3}$)	($g \cdot cm^{-3}$)	(%)	μm	(HV0.01)	(HV0.5)	(HRC)
0C	0.012	4.507	4.509	99.96	0.102	431	262	24.3
20C	0.024	4.433	4.508	98.34	0.055	497	299	29.6
50C	0.084	4.350	4.503	96.61	0.075	504	352	35.7
100C	0.346	4.326	4.482	96.52	0.091	535	363	36.9

[1] Archimedes method

[2] Rule of mixture; using: ρ Ti = 4.51 $g \cdot cm^{-3}$ and ρ MWCNTs = 1.6 $g \cdot cm^{-3}$

Hardness at the surface and in the bulk of materials was measured using a micro-Vickers hardness tester in scale HV0.01 (98.07mN) and HV0.5 (4.90N), as shown in **Fig. 2.** Bulk hardness directly increased with increasing MWCNT content. Regarding the effect of TiH compounds on hardness, previous work showed that the micro-hardness of TiH was about 30% higher than that of pure Ti[16]. In the case of the 0C and 100C specimens, the bulk hardness value was 28% different, which should be mainly affected by MWCNTs rather than TiH. Thus, greater bulk hardness was created by a high distribution of MWCNTs and their TiC products in the Ti matrix. The surface hardness showed a higher value than bulk hardness because an oxide layer was formed on the surface. The oxide layer also causes a reduction of the friction coefficient, as mentioned below.

3.2 Observation of Sliding

Damaged surfaces were investigated using optical and scanning electron microscopy in an attempt to understand the wear behavior.

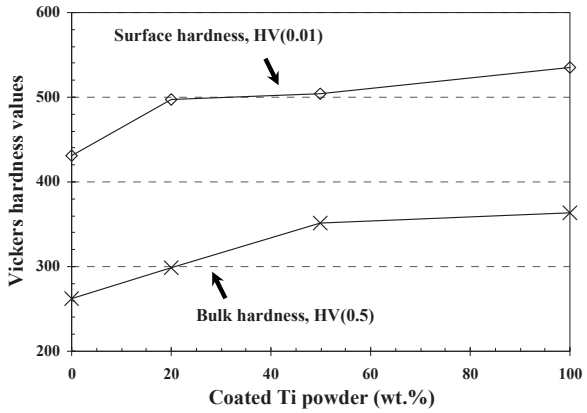

Fig.2 Dependence of the bulk hardness and surface hardness of composite materials on the amount of MWCNTs-coated Ti powder.

Figure 3 shows the overall sliding surfaces of the 0C and 100C samples after wear test with a 2.94N applied load. White and black areas correspond to adhesive and abrasive regions. Notably, the severe adhesive area occurred in the case of the 0C sample (**Fig. 3(a)**) and decreased with an increasing amount of coated Ti powder (20C, 50C and 100C). In contrast to the abrasive area, which remarkably occurred in 100C (**Fig. 3(c)**) because of the abrasive particulates such as the hard TiC particles that formed at the outer boundary of the MWCNTs, which easily fractured during testing. Debris is diversified in shape and size, as shown in **Fig. 3(d)**. High magnification observation of the debris is shown in **Fig. 4**.

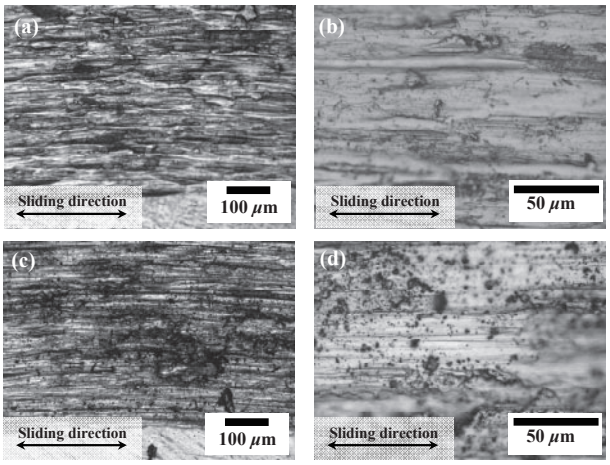

Fig.3 Observation of sliding surfaces of a 0C specimen (pure Ti) (a)-(b) and a 100C specimen (c)-(d) after wear testing.

It clearly reveals the remaining MWNCTs surrounded by TiC compounds/Ti particles. Figure 4(b) shows that deformed MWCNT thin films could be considered as solid lubricating films able to lower the friction coefficient. This is one reason why the severe adhesive wear area decreased with increasing the MWCNT content of the composite. EDS-point analysis was applied to the worn surface (**Fig. 4(a)**) and debris (**Fig. 4(b)**).

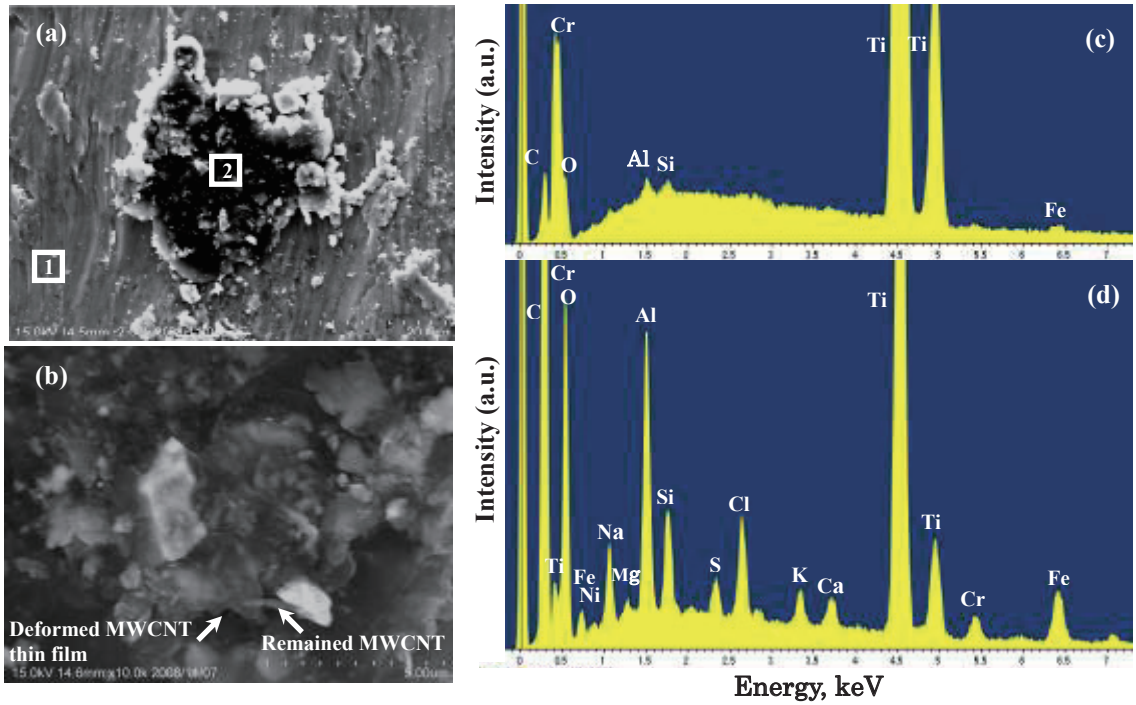

Fig. 4 SEM-EDS results of a worn surface of a 100C specimen. Overview of worn surface (a), high magnification around marker No.2 (b), EDS results of marker No. 1 (c) and marker No.2 (d)

As shown in **Fig. 4(c)**, the sliding surface of **Fig. 4(a)** mainly contained Ti, Cr, Al, Fe, C and O. In contrast, in **Fig. 4(d)**, the main peaks consisted of Ti, Ca, O, Cr, Al, Fe, Ni and Na. Elemental Fe, Cr and Ni were detected from the 304 stainless steel ball, and other elements resulted from the zwitterionic solution and impurities of the MWCNTs themselves.

The tribochemical reactions of the worn surface were not characterized at this stage. Structure and phase confirmation of the sliding surface were characterized by locally selected XRD. The patterns shown in **Fig. 5** correspond to the worn surfaces of the 0C and 100C specimens. They showed only three phases, consisting of Ti, TiC and TiH. There were no detected TiO2 peaks, which is inconsistent with EDS results. The lack of TiO2 peaks in the XRD patterns is because the TiO2 peaks coincide with the Ti diffraction peaks.

3.3 Friction coefficient

Changes in friction coefficient profiles (sliding distance of 18.85 m) of the 100C and 0C compositions with different applied loads are shown in Figs. 6 and 7, respectively. The friction coefficient profiles of the 100C specimen obviously showed low and high regions during testing, as presented by **Fig. 6**. The low friction coefficient occurred at the first period of the test and gradually decreased with an increasing applied load. The results of the 50C sample are almost the same as those in the case of the 100C specimen (**Fig. 6**).

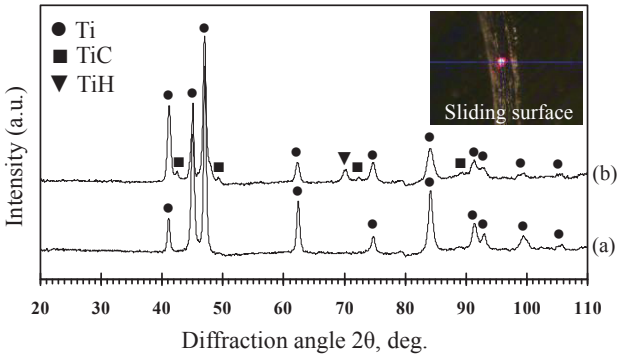

Fig. 5 X-ray diffraction analysis on sliding surfaces of 0C specimen (a) and a 100C specimen (b).

The low friction behavior of the 50C and 100C specimens demonstrated that any applied load could not immediately break down the oxide layer at the onset of testing. The oxide layer hardness is implicitly expressed by the surface hardness results shown in **Fig. 2**. After the oxide layer broke down, the sliding contacts between the SUS304 ball and the disk specimen directly touched together and suddenly increased the friction coefficient. On the other hand, the 0C composition does not show a low friction coefficient region, as seen in **Fig.7**. The frictional profiles of the 0C sample at a 0.98N load showed stronger stick amplitude compared with higher applied loads. It showed that adhesive wear dominated at a low applied load and changed to abrasive wear when the applied load was increased.

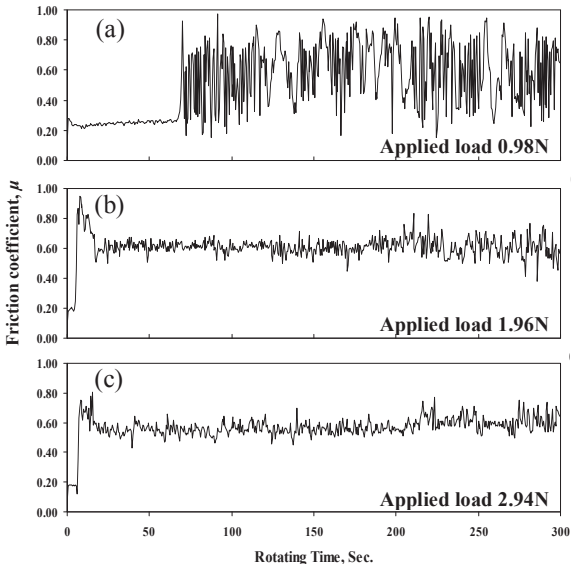

Fig. 6 Friction coefficient profiles of a 100C specimen under different applied loads of 0.98N (a), 1.96N (b) and 2.94N (c).

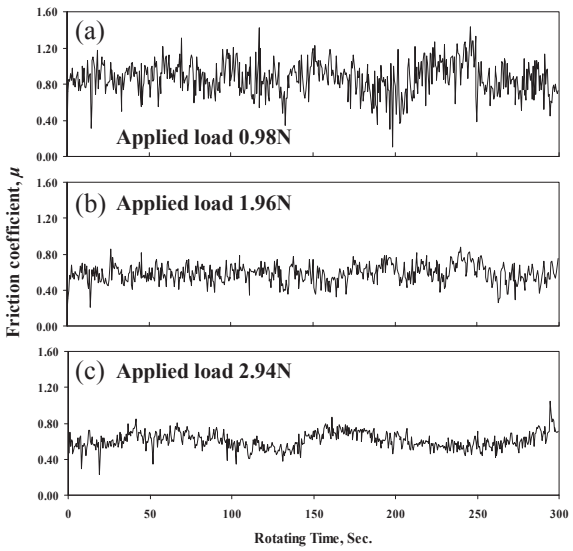

Fig. 7 Friction coefficient profiles of a 0C specimen under different applied load of 0.98N (a), 1.96N (b) and 2.94N (c).

This behavior also showed the same trend in the 100C specimen. For the evaluation of the kinetic friction coefficient of each composition, shown in Fig. 8, it is effective to neglect the low friction coefficient region. The average kinetic friction coefficient gradually decreases with increasing MWCNT-coated Ti powder content except for the composition of 100C. The increasing kinetic friction coefficient of the 100C specimen is believed to be from abrasive wear fragments that are recombined between themselves and/or remained MWCNTs, shown in **Fig. 4(a)**, resulting in a retardation of counterpart sliding.

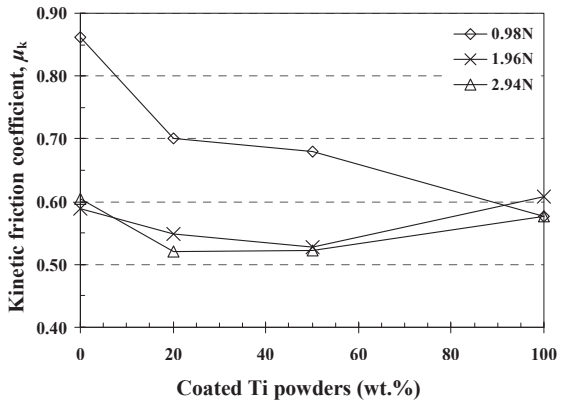

Fig.8 Kinetic friction coefficient (μ_k) of each composition at different applied loads.

4. Conclusions

(1) The remarkable enhancement of hardness is due to a homogeneous distribution of MWCNTs and TiC compounds in the Ti matrix.

(2) The remaining MWCNTs showed good self-lubricating properties, resulting in a lower friction coefficient.

(3) An adhesive phenomenon of pure Ti reinforced with MWCNTs dominated the wear behavior when using a low applied load, while abrasive wear dominated wear processes at high applied loads.

References

1) Iijima S. Helical microtubules of graphitic carbon. Nature 1991; 354: 56-58.
2) Iijima S, Brabec C, Maiti A, Bernholc J. Structural flexibility of carbon nanotubes. J. Chem. Phys. 1996; 104: 2089-2092.
3) Falvo MR, Clary GJ, Taylor II RM, Chi V, Brooks Jr FP, Washburn S, Superfine R. Bending and buckling of carbon nanotubes under large strain. Nature 1997; 389: 582-584.
4) Kuzumaki T, Ujiie O, Ichinose H, Ito K. Mechanical characteristics and preparation of carbon nanotube fiber-reinforced Ti composite. Adv. Eng. Mater. 2000; 2: 416-418.
5) George R, Kashyap K.T, Rahul R, Yamdagni S. Strengthening in carbon nanotube/aluminum (CNT/Al) composites. Script. Mat. 2005; 53: 1159-1163.
6) Quang P, Jeong YG, Yoon SC, Hong SH, Kim HS. Consolidation of 1 vol.% carbon nanotube reinforced metal matrix nanocomposites via equal channel angular pressing. J. Mater. Proc Tech. 2007; 187-188: 318-320.
7) Shimizu Y, Miki S, Soga T, Itoh I, Todoroki H, Hosono T. Sakaki K, Hayashi T, Kim YA, Endo M, Morimoto S, Koide A. Multi-walled carbon nanotube-reinforced magnesium alloy composites. Script. Mat. 2008; 58: 267-270.
8) Kondoh K, Threrujirapapong T, Imai H, Umeda J, Fugetsu B. CNTs/TiC reinforced titanium matrix nanocomposites via powder metallurgy and its microstructural and mechanical properties. J. of Nanomaterials, vol. 2008, Article ID 127538, 4 pages, 2008.

9) Kim KT, Cha SI, Hong SH. Hardness and wear resistance of carbon nanotube reinforced Cu matrix nanocomposites. Mater. Sci. Eng. A 2007; 449-451: 46-50.
10) Miyoshi K, Sanders JH, Hager Jr. C.H, Zabinski JS, Vader Wal RL, Andrews R, Street Jr. KW, Lerch BA, Abel PB. Wear behavior of low-cost, lightweight TiC/Ti-6Al-4V composite under fretting: Effectiveness of solid-film lubricant counterparts. Tribology Int 2008; 41(1): 24-33.
11) Umeda J, Kondoh K, Imai H. Friction and wear behavior of sintered magnesium composite reinforced with CNT-Mg¬2Si/MgO. Mater. Sci. Eng. A 2009; 504: 157-162
12) Cumings J, Zettle A. Low-friction nanoscale linear bearing realized from multiwall carbon nanotubes. Science 2000; 289: 602-604.
13) Fugetsu B, Han W, Endo N, Kamiya Y, Okkuhara T. Disassembling single-walled carbon nanotube bundles by dipole/dipole electrostatic interactions. Chem. Lett. 2005; 34: 1218-1219.
14) Lee W, Shin H, Lee WY. Microstructural evolution during the hot-pressing of TiH2-TiC particle mixtures. Script. Mat. 2003; 48: 719-724.
15) Leyens C, Peters M. Titanium and Titanium Alloys. Wiley-VCH, 2003.
16) Xu JJ, Cheung HY, Shi SQ. Mechanical properties of titanium hydride. J. Alloy. Compd. 2007; 436: 82-85